






Article

In Vitro and In Vivo Studies of Biodegradability and Biocompatibility of Poly(ϵ CL)-*b*-Poly(EtOEP)-Based Films

Ilya Nifant'ev ^{1,2,3,*}, Andrey Shlyakhtin ¹, Pavel Komarov ², Alexander Tavtorkin ², Evgeniya Kananykhina ⁴, Andrey Elchaninov ⁵, Polina Vishnyakova ⁵, Timur Fatkhudinov ^{4,6} and Pavel Ivchenko ^{1,2}

¹ Chemistry Department, M.V. Lomonosov Moscow State University, 1-3 Leninskie Gory, 119991 Moscow, Russia; shlyakhtinav@mail.ru (A.S.); phpasha1@yandex.ru (P.I.)

² A.V. Topchiev Institute of Petrochemical Synthesis RAS, 29 Leninsky Pr., 119991 Moscow, Russia; komarrikov@yandex.ru (P.K.); tavgorkin@yandex.ru (A.T.)

³ Faculty of Chemistry, National Research University Higher School of Economics, 20 Miasnitskaya Str., 101000 Moscow, Russia

⁴ Research Institute of Human Morphology, 3 Tsyurupy St., 117418 Moscow, Russia; e.kananykhina@gmail.com (E.K.); tfat@yandex.ru (T.F.)

⁵ National Medical Research Center for Obstetrics Gynecology and Perinatology Named after Academician V.I. Kulakov of Ministry of Healthcare of Russian Federation, 4 Oparina Str., 117997 Moscow, Russia; elchandreya@yandex.ru (A.E.); vpa2002@mail.ru (P.V.)

⁶ Department of Histology, Cytology and Embryology, Peoples' Friendship University of Russia, Miklukho-Maklaya 6 Str., 117198 Moscow, Russia

* Correspondence: ilnif@yahoo.com or inif@org.chem.msu.ru; Tel.: +7-495-939-4098

Received: 8 December 2020; Accepted: 17 December 2020; Published: 18 December 2020



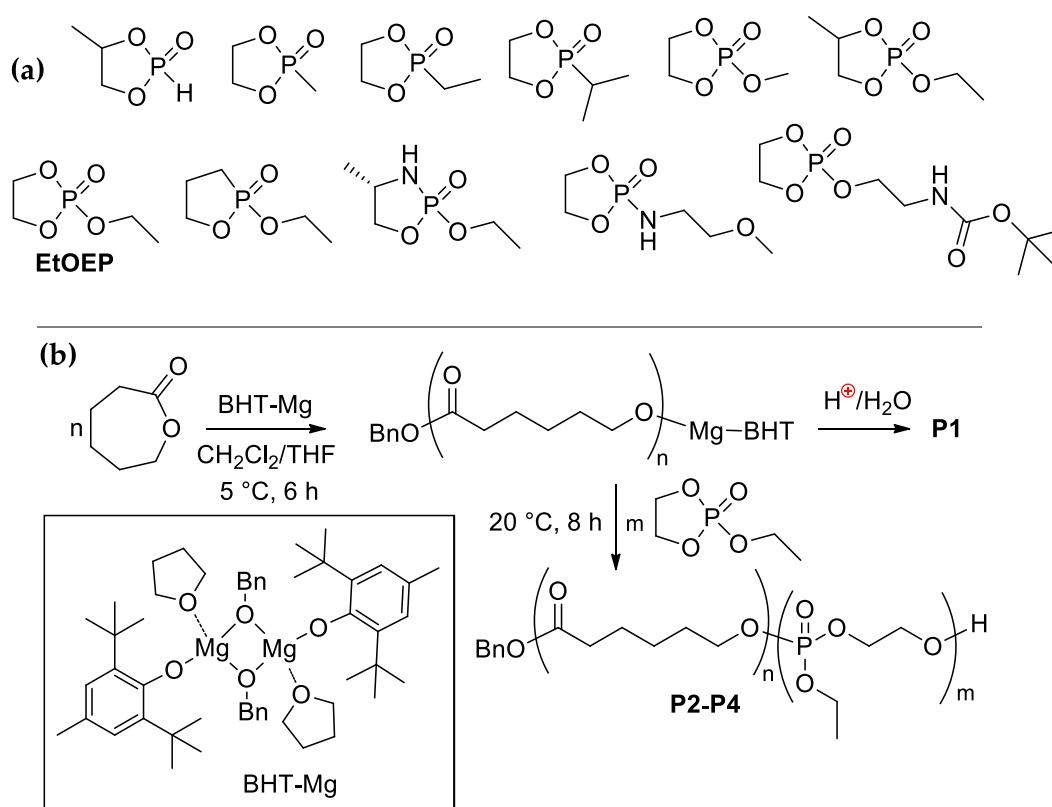
Abstract: The control of surface bioadhesive properties of the subcutaneous implants is essential for the development of biosensors and controlled drug release devices. Poly(alkyl ethylene phosphate)-based (co)polymers are structurally versatile, biocompatible and biodegradable, and may be regarded as an alternative to poly(ethylene glycol) (PEG) copolymers in the creation of antiadhesive materials. The present work reports the synthesis of block copolymers of ϵ -caprolactone (ϵ CL) and 2-ethoxy-1,3,2-dioxaphospholane-2-oxide (ethyl ethylene phosphate, EtOEP) with different content of EtOEP fragments, preparation of polymer films, and the results of the study of the impact of EtOEP/ ϵ CL ratio on the hydrophilicity (contact angle of wetting), hydrolytic stability, cytotoxicity, protein and cell adhesion, and cell proliferation using umbilical cord multipotent stem cells. It was found that the increase of EtOEP/ ϵ CL ratio results in increase of hydrophilicity of the polymer films with lowering of the protein and cell adhesion. MTT cytotoxicity test showed no significant deviations in toxicity of poly(ϵ CL) and poly(ϵ CL)-*b*-poly(EtOEP)-based films. The influence of the length of poly(EtOEP)chain in block-copolymers on fibrotic reactions was analyzed using subcutaneous implantation experiments (Wistar line rats), the increase of the width of the fibrous capsule correlated with higher EtOEP/ ϵ CL ratio. However, the copolymer-based film with highest content of polyphosphate had been subjected to faster degradation with a formation of developed contact surface of poly(ϵ CL). The rate of the degradation of polyphosphate in vivo was significantly higher than the rate of the degradation of polyphosphate in vitro, which only confirms an objective value of in vivo experiments in the development of polymer materials for biomedical applications.

Keywords: polyesters; polyphosphoesters; polycaprolactone; protein adsorption; ring-opening polymerization; cytotoxicity; immunohistochemical test

1. Introduction

The prevention of unspecific protein adsorption and cell interactions, which can lead in vivo to a foreign body reaction, is important in developing new biomaterials which are in direct contact with body tissues, such as implants, prosthetics, biosensors, controlled drug release devices [1]. Initial nonspecific protein adsorption on the surface of the implant supports the formation of fibrous capsule, a diffuse barrier for drug release and blood penetration to biosensors [2]. The development of the materials with anti-adhesive properties is of great relevance. Since poor protein resistance is often associated with surface hydrophobicity, efficient way to such materials is a modification of the surface by poly(ethylene glycol) (PEG) [1,3,4]. However, low biodegradability of PEG causes formation of PEG antibodies, emergence of hypersensitivity, etc. [5]. In some experiments with subcutaneous injection of PEGylated implants, the formation of fibrous capsule was detected [6]. Consequently, the search of PEG alternative for ‘hydrophilization’ of the surface of the implants is still relevant for the chemistry of biodegradable polymers.

Ethylene phosphates, phosphonates and phosphoramidates with short alkyl substituents (Scheme 1a) represent promising cyclic substrates for the synthesis of copolymers with hydrophilic biodegradable blocks using catalytic ring-opening polymerization (ROP, Scheme 1b) [5,7–14]. 2-Ethoxy-1,3,2-dioxaphospholane 2-oxide (ethyl ethylene phosphate, EtOEP) is one of the most reliable monomers for the preparation of hydrophilic polyphosphoesters (PPEs) due to high reactivity and low tendency to form branched polymers [15–17]. Block copolymers poly(ϵ CL)-*b*-poly(EtOEP) were synthesized previously using tin (II) octanoate as a catalyst [15].



Scheme 1. (a) Cyclic phosphorus-containing monomers suitable for the synthesis of water-soluble biodegradable polymers [5]; (b) Synthesis of poly(ϵ CL) and poly(ϵ CL)-*b*-poly(EtOEP).

The main part of the works on biomedical application of PPEs and related polymers is related to drug and gene delivery [7,9,10,12,18–22], there were only few studies dealing with the use of PPEs

for the surface modification [5,23,24]. As far as we know, the influence of the surface modification by PPEs on immune response have not been studied to date.

Taking into account possible toxicity of tin (II) derivatives [25], it seems preferable to use coordination catalysts, based on 'biometals' (Na, Mg, Ca, Al, Zn), in the preparation of polymers for biomedical applications. In the present paper, the synthesis of ϵ CL homopolymer **P1** and block-copolymers poly(ϵ CL)-*b*-poly(EtOEP) **P2–P4** with $DP_n(\epsilon\text{CL}) \sim 200$ and different $\epsilon\text{CL}/\text{EtOEP}$ ratios (~ 32 , ~ 8 and ~ 3 , respectively) by living ROP of ϵCL and EtOEP, initiated by non-toxic complex [(BHT)Mg(μ -OBn)(THF)]₂ (BHT-Mg) [26] (Scheme 1b) followed by the preparation of polymer films, is reported. These films were studied in vitro with a view to evaluating the impact of EtOEP/ ϵCL ratio on the hydrophilicity, hydrolytic stability, cytotoxicity, protein and cell adhesion, and cell proliferation using umbilical cord multicomponent stem cells (UC MSCs). For the first time for PPE-containing materials, in vivo subcutaneous implantation experiments using Wistar rats were performed.

2. Materials and Methods

2.1. Synthesis of (co)Polymers

2.1.1. General Experimental Remarks

All of the synthetic and polymerization experiments were performed under a purified argon atmosphere. CH_2Cl_2 was washed with aqueous Na_2CO_3 , stirred with CaCl_2 powder, refluxed over CaH_2 for 8 h and distilled. Tetrahydrofuran (THF) and diethyl ether (Et_2O) (Merck, Darmstadt, Germany) were refluxed with Na/benzophenone and distilled prior to use. ϵCL (Merck, Darmstadt, Germany) was distilled prior to use under argon over CaH_2 . Ethyl ethylene phosphate (EtOEP) [27] and BHT-Mg [26] were synthesized according to the literature procedures.

CDCl_3 (D 99.8%, Cambridge Isotope Laboratories, Inc., Tewksbury, MS, USA) was distilled over P_2O_5 and stored over 4 Å molecular sieves. The ^1H (400 MHz) and ^{31}P (162 MHz) NMR spectra were recorded on a Bruker AVANCE 400 spectrometer (Bruker, Billerica, MS, USA) at 20 °C. The chemical shifts were reported in ppm relative to the solvent residual peak ($\delta = 7.26$ ppm).

Size exclusion chromatography (SEC) was performed on an Agilent PL-GPC 220 chromatograph (Agilent Technologies, Santa Clara, CA, USA) equipped with a PLgel column, using THF as an eluent (1 mL/min). The measurements were recorded with universal calibration according to polystyrene standards at 40 °C.

2.1.2. Synthesis of Poly(ϵCL) **P1**

ϵCL (3.82 mL, 34.5 mmol) was placed into flame-dried vial, equipped with magnetic stirrer bar and septum. CH_2Cl_2 (11.7 mL) was added, the solution was cooled to 5 °C, the solution of BHT-Mg (73 mg, 0.17 mmol) in THF (2.0 mL) was added. After 6 h of stirring at 5 °C, AcOH (52 μL) was added. The solvents were removed under reduced pressure, the residue was dried in vacuo, dissolved in CH_2Cl_2 (60 mL). The solution of poly(ϵCL) was washed by 1M HCl (30 mL), distilled water (2×30 mL), dried over MgSO_4 , and filtered. The solution was evaporated and poured into Et_2O . The yield was 2.45 g (62%).

End-group analysis of ^1H NMR spectra of **P1** (see Figure S1 in the Supplementary Materials) was used for the determination of M_n^{NMR} by comparative integration of the signals of poly(ϵCL) protons and aromatic protons of benzyl group at 7.3–7.4 ppm.

2.1.3. Synthesis of Poly(ϵCL)-*b*-Poly(EtOEP) **P2–P4**

ϵCL (3.82 mL, 34.5 mmol) was placed into flame-dried vial, equipped with magnetic stirrer bar and septum. CH_2Cl_2 (11.7 mL) was added, the solution was cooled to 5 °C, the solution of BHT-Mg (73 mg, 0.17 mmol) in THF (2.0 mL) was added. After 6 h of stirring at 5 °C, calculated quantities of EtOEP (20, 40 and 60 equivalents relatively to BHT-Mg, 410, 820, and 1230 μL for the synthesis of **P2**, **P3** and **P4**,

respectively) were added, the reaction mixtures were stirred for 10 min at 5 °C. Then, AcOH (52 µL) was added. The solvents were removed under reduced pressure, the residue was dried in vacuo, dissolved in CH₂Cl₂ (80 mL). The solutions were shaken with 1M HCl, the emulsions were evaporated under reduced pressure, polymer residues were separated by filtration, and dissolved in CH₂Cl₂. This procedure was repeated with H₂O. The polymers obtained were dried at 0.02 Torr to constant weight. The residues were dissolved in dimethoxymethane (minimal amount) and poured into Et₂O with a separation of the polymer precipitates. This procedure was repeated once. The products were dried in vacuo and analyzed. The yields were 2.94 g (66%) for **P2**, 2.89 g (58%) for **P3**, 2.86 g (52%) for **P4**.

M_n^{NMR} was determined by comparative integration of the signals of poly(εCL) protons, poly(EtOEP) protons and aromatic protons of benzyl group in ¹H NMR spectra of the copolymers (see Figures S2–S4 in the Supplementary Materials).

2.2. Preparation and Mechanical Testing of Polymer Films

Polymer films for mechanical testing **FM1–FM4** (film thickness 0.16–0.17 mm) were prepared using HLCL-1000 hot melt coater/laminator (ChemInstruments, Fairfield, OH, USA). Dog-bone tensile specimens (ASTM standard D1708-96, 22 × 5 mm) were prepared by punching the films from a stainless steel die. A I1140M-5-01-1 universal tensile testing machine (Tochpribor-KB, Ivanovo, Russia) and ASTM D638 method were used for film mechanical testing.

2.3. Preparation of Polymer Films for Hydrolytic and Biomedical Testing

2.3.1. Preparation of Polymer Films

Polymer films for biomedical testing **FB1–FB4** were prepared by dissolution of 300 mg of polymers **P1–P4** in CH₂Cl₂ (4 mL), followed by slow evaporation of the solution in Petri dishes (6 cm diameter). Copolymer **P4** was also used in preparation of the sample **FB4'** with higher film thickness by dissolution of 1.00 g of **P4** in CH₂Cl₂ (6 mL) followed by slow evaporation in Petri dish (6 cm diameter).

2.3.2. Contact Angle Measurements

For the determination of hydrophilicity of the films, the static contact angle of distilled water on the surface of the films **FB1–FB4** was measured using a LK-1 goniometer equipped with a CCD camera (RPC OpenScience Ltd., Krasnogorsk, Russia) for both surfaces, smooth (film side that was in contact with glass) and rough (film side that was in contact with air during evaporation of the polymer solution). The images of water drops on the sample surface were analyzed with software supplied by the manufacturer. Ten samples were measured in each type of the films. Initially, distilled water (5 mL) was used in each measurement after exposure for 3 s at ambient temperature and 70% relative humidity.

2.3.3. Hydrolytic Degradation in Vitro

Huber MPC-E immersion thermostat (Huber Kältemaschinenbau, Offenburg, Germany) was used in experiments on hydrolytic polymer degradation in PBS that were performed by the common method [28,29]. The temperature of hydrolysis was 39 °C (normal temperature of the rat body, to compare with the results of the experiments in vivo). Given the stability of poly(εCL) blocks against degradation under mild conditions, the residual content of poly(EtOEP) fragments was analyzed using ¹H NMR spectroscopy.

Scanning electron microscope (SEM) images of the polymer surfaces were obtained using a JEOL JSM-6000PLUS Neoscope II (Jeol Ltd., Tokyo, Japan) at the accelerating voltage of 15.0 kV.

2.3.4. Preparation of the Samples for Biomedical Testing

Phosphate-buffered saline (PBS) containing 0.131 mol/L NaCl and 0.0027 mol/L KCl (Merck, Darmstadt, Germany) was used as purchased. For biomedical studies, the samples of **FB1–FB4** and **FB4'** were placed to 96% and 70% ethanol (20 min exposition in each solution) for wetting and sterilization, ethanol was removed by exposition in PBS (3 × 5 min). Finally, the film samples were exposed for 1 h in culture medium.

2.4. Protein Adhesion

The samples of **FB1–FB4** were incubated for 18 h at 4 °C in PBS containing green fluorescent protein (GFP; Evrogen, Moscow, Russia) with a concentration of 0.2 mg/mL, washed three times by PBS and studied using a Leica DM 4000 fluorescent microscope (Leica Microsystems GmbH, Wetzlar, Germany).

2.5. Cultivation of UC MSCs

Based on the data compiled and reported earlier [30,31], UC MSCs were isolated using fermentation from Wharton's jelly of umbilical cord. Collecting of umbilical cord was approved by the Commission of Biomedical Ethics at National Medical Research Center for Obstetrics, Gynecology and Perinatology of Ministry of Healthcare of Russian Federation, Moscow (ethics committee approval protocol no. 12, 17 November 2016). Written informed consent was obtained from all participants prior to the study. UC MSCs were cultured in Dulbecco's Modified Eagle Medium F-12 (DMEM-F12) (PanEco, Moscow, Russian Federation) containing 10% fetal bovine serum (FBS; PAA Laboratories, Linz, Austria) at 37 °C under 5% CO₂ humidified atmosphere. Belonging of the cell culture to MSCs was confirmed by the estimation of the expression of positive (CD90, CD105) and negative (CD34, CD45) markers as well as possibility of induced cell differentiation in osteogenic, chondrogenic and adipogenic directions *in vitro*.

UCMSCs were seeded to the surface of film samples and cultured at 37 °C under 5% CO₂ humidified atmosphere. The samples (three for each type of polymer **FB1–FB4**) were transferred to bioreactor vials (SPL Life Sciences, Pocheon, Korea) containing 5 mL of cell suspension (8×10^5 cells total). The vials were placed into orbital shaker (BioSan, Riga, Latvia), placed to CO₂ incubator. Cell cultivation was carried out during 24 h at 75 rpm and then during 48 h at 50 rpm.

2.6. Cell Visualization and Count

For cell visualization and cell count on the surface of polymer films, UC MSCs seeded samples were fixed in 4% paraformaldehyde at 0 °C, then the cell nuclei were stained with DAPI (Merck, Darmstadt, Germany) following the manufacturer's protocol.

Additionally, to observe the cell morphology on the surface of the films, the cells were labeled with a fluorescent red-orange vital dye PKH26 (Merck, Darmstadt, Germany) before settling the samples, according to manufacturer's recommendations.

2.7. Cytotoxicity Studies

Quantitative assessment of the cytotoxic properties of the films was obtained using a standard MTT test with an incubation period of one, two, and four days. UC MSCs were seeded to the surface 96-well culture plate at a density of 7.0×10^3 cells/well (70% confluence) and cultured in growth medium at 37 °C under 5% CO₂ humidified atmosphere. Then 20 µL MTT (Merck, Darmstadt, Germany; 5 mg/mL) was added to each well of the plate and the plates were incubated at 37 °C for additional 2 h. The supernatants were removed, and 50 µL DMSO was added to each well. Absorbance was measured at $\lambda = 570$ nm on a Multiskan GO Spectrophotometer (Thermo Fisher Scientific, Waltham, MS, USA).

2.8. Immunocytochemical Studies

UC MSCs seeded samples were treated with Hanks' Balanced Salt solution (Merck, Darmstadt, Germany), fixed by 4% paraformaldehyde (5 min) and by cold methanol (1 min), and stained with antibodies ab15580 (Abcam, Cambridge, UK) against proliferation marker Ki-67 according to manufacturer's recommendations. The second type of antibodies was PE-conjugated sc3739 (Santa Cruz Biotechnology, Dallas, TX, USA), cell nuclei were stained with DAPI (Merck, Darmstadt, Germany). The observations were carried out with the use of a Leica DM 4000 B fluorescent microscope and LAS AF v.3.1.0 build 8587 software (Leica Microsystems GmbH, Wetzlar, Germany).

2.9. Subcutaneous Implantation Experiments

2.9.1. Animals

Outbred, eight-week-old male Wistar rats (250–300 g) were obtained from the Institute for Bioorganic Chemistry branch animal facilities (Pushchino, Moscow, Russia). All experimental work involving animals was carried out according to the Standards of Laboratory Practice (National Guidelines No. 267 by Ministry of Healthcare of the Russian Federation, 1 June 2003), and all efforts were made to minimize suffering. The animals were adapted to laboratory conditions (23 °C, 12 h/12 h light/dark, 50% humidity, ad libitum access to food and water) for two weeks prior to manipulation.

2.9.2. Subcutaneous Administration of the Polymer Films

All manipulations with animals were carried out in accordance with 'Rules for carrying out work using experimental animals' (order of the USSR Ministry of Health No. 755 dated 12.08.1977) after approval by Ethical Review Board at the Scientific Research Institute of Human Morphology (Protocol no. 10, 4 October 2019). The experiment was performed using 28 male rats of the Wistar line (mass of body 200–250 g). The animals were anesthetized using an intramuscular injection of zoletil (at the rate of 10 mg/kg) and medetin (at the rate of 0.12 mg/kg). In rats, hair was shaved off in the interscapular area, fixed on the operating table, and the operating field was treated with 70% alcohol. With scissors, a skin incision was made in the interscapular region, pockets were made bluntly on each side of the incision under the skin, where the sample of the polymer film (0.7 cm diameter) was inserted, the skin was sutured with interrupted sutures (Figure 1), and the wound was treated with 70% alcohol. By the number of the films under study (**FB1–FB4** and **FB4'**), the rats were divided into five groups, containing four rats for each **FB1–FB4** and **FB4'** implants.



Figure 1. Subcutaneous administration of the polymer films.

2.9.3. Morphometric Studies

After 14 days (**FB4** and **FB4'** implants) and 28 days (all implants) the rats were taken out from the experiment by euthanasia in a CO₂-chamber. The capsule with the implant was excised, and fixed in 10% formaldehyde solution within 72 h. The tissue samples were encased in paraffin. To study

morphological changes, cross sections of 7 μm thick were made using rotary microtome Accu-Cut SRM (Sakura Finetek, Tokyo, Japan). The sections were stained by hematoxylin and eosin, dehydrated and enclosed in a synthetic mounting medium (BioVitrum, Saint-Petersburg, Russia).

Morphometric studies were carried out on the micrographs of the samples, stained by hematoxylin and eosin, using a Leica DM 2500 microscope and ImageScope M software (Leica Microsystems GmbH, Wetzlar, Germany) (Figure S5 in the Supplementary Materials). For each experiment, six sections were randomly selected and micrographs were made for 10 fields of view on each histological section.

2.9.4. Immunohistochemical Studies

A part of the samples was fixed using liquid nitrogen. Cryosections of 5–7 μm thickness were made using cryotom Leica CM1900 (Leica Microsystems GmbH, Wetzlar, Germany), and SuperFrost glass slides (Menzel, Germany). The sections were stained with ab125212 antibodies (Abcam, Cambridge, UK) against the macrophage marker CD68; cell nuclei were stained by DAPI. To estimate the quantity of CD68+ cells, micrographs at 400 \times magnification (Leica DM 4000 B microscope) were analyzed.

2.10. Statistical Analysis

The data is presented as the mean \pm standard deviation (SD) and median with interquartile range. One-way ANOVA followed by Dunnett's multiple comparisons test was performed using Sigma Stat 3.5 (Systat Software, San Jose, CA, USA). Values of $p < 0.05$ were considered statistically significant.

3. Results and Discussion

3.1. Polymerization and (co)Polymer Characteristics

As was demonstrated previously, BHT-Mg catalyst is highly efficient in living ROP of cyclic substrates such as cyclic esters [26,32] and CEPMS [11,33–37]. In our experiments (Table 1), ϵCL homopolymer **P1** and $\epsilon\text{CL}/\text{EtOEP}$ block copolymers **P2–P4** were obtained using consecutive low-temperature polymerization of ϵCL and EtOEP. The living character of BHT-Mg initiated polymerization of ϵCL and EtOEP was proved by the consistency of $\epsilon\text{CL}/\text{EtOEP}$ ratios in copolymers formed and in copolymers separated after a series of successive re-precipitations. These data were obtained by the analysis of NMR spectra of the reaction mixtures and copolymers after separation (see Section S1 in the Supplementary Materials).

3.2. Mechanical Properties of Polymers

The tensile strength properties of the films **FM1–FM4** were examined at 25 $^{\circ}\text{C}$ using standard method (see Section 2.2), and the results are illustrated in Table 2. Poly(ϵCL) film **FM1** demonstrated highest tensile strength and elongation, these parameters showed a downward trend with an increasing of EtOEP content in block copolymers, in the transition from **FM2** to **FM4**. At the same time, **FM2** had the highest Young's modulus among polymers studied. Based on mechanical test, copolymer film **FM4** with the highest EtOEP content must be recognized as not usable for the producing of biopolymer scaffolds.

Table 1. Polymerization experimental data for BHT-Mg catalyzed (co)polymerization. Reaction conditions: CH₂Cl₂/THF, [εCL] = 2 M.

Run	εCL/EtOEP/BHT-Mg Initial Ratio	εCL Conv., % ¹	EtOEP Conv., % ¹	Polymer Composition DP _n (εCL)/ DP _n (EtOEP) ²	M _n ^{theo} × 10 ^{3 3}	M _n ^{NMR} × 10 ^{3 2}	M _n ^{SEC} × 10 ^{3 4}	D _M ⁴
P1 ⁶²⁸	200/–/1	>99	—	—	22.9	30.0	36.0	1.38
P2	200/20/1	>99	83	31.6	25.2	34.9	32.7	1.81
P3	200/40/1	>99	92	8.3	27.9	31.3	28.8	2.00
P4	200/60/1	>99	87	2.8	32.4	32.6	46.5	2.04

¹ DP_n (degree of polymerization) was determined by the analysis of the NMR spectra of the reaction mixtures. ² M_n^{theo} = n × M(εCL) + m × M(EtOEP) + M(BnOH), where n and m are the numbers of εCL and EtOEP fragments determined by comparative integration of the signals of BnO group (δ ~7.3 ppm, 5H) and signals of CH₂O fragments of εCL (δ = 4.05 ppm, 2nH) and EtOEP (δ = 4.15–4.30 ppm, 6mH). ³ M_n^{theo} = M(εCL) × Conv. (εCL) + M(EtOEP) × Conv. (EtOEP) + M(BnOH). ⁴ Determined by size exclusion chromatography (SEC) in THF vs. polystyrene standards and corrected by the factor of 0.56.

Table 2. Tensile properties of polymer films.

Polymer	Average Cross-Sectional Area, mm ²	Tensile Strength, MPa	Yield Stress σ, MPa	Young's Modulus E, MPa	Elongation at Break ε _p , %
FM1	0.81	20.2 ± 9.6	14.5 ± 0.6	207 ± 19	72 ± 78
FM2	0.84	11.9 ± 5.0	16.6 ± 0.7	251 ± 20	455 ± 147
FM3	0.82	9.5 ± 6.2	14.8 ± 0.5	200 ± 39	515 ± 100
FM4	0.82	4.0 ± 1.4	6.3 ± 2.0	163 ± 68	4.0 ± 0.8

3.3. Hyrdophilicity and Hydrolysis In Vitro

3.3.1. The Results of the Contact Angle Measurements

As was to be expected, the $\epsilon\text{CL}/\text{EtOEP}$ ratio has a direct impact on the contact angle values (Figure 2). Increasing of EtOEP content resulted in lowering of the contact angle; the films **FB3** and **FB4** can be considered as highly hydrophilic.

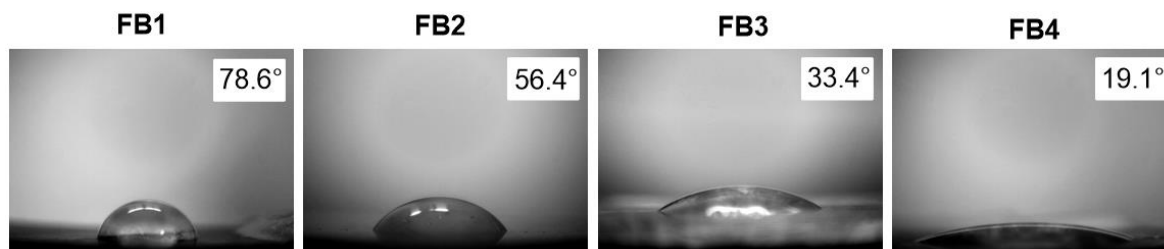


Figure 2. Contact angles of wetting for **FB1**–**FB4**.

3.3.2. Hydrolytic Degradation in Buffer Solution

To study in vitro hydrolytic degradation behavior we exposed 200 mg samples of **FB1**–**FB4** films with PBS at pH 7.4 and 37.0 ± 0.1 °C for 14 days. The morphologies of **FB4** films before and after hydrolysis were first characterized by SEM. Essential results were obtained for **FB4** film. The SEM results show that the topological structure of the **FB4** film before hydrolysis had no fibers and the surface was relatively smooth (Figure 3a). However, after 14 days the surface morphology has changed significantly with a formation of multiple caverns (Figure 3b).

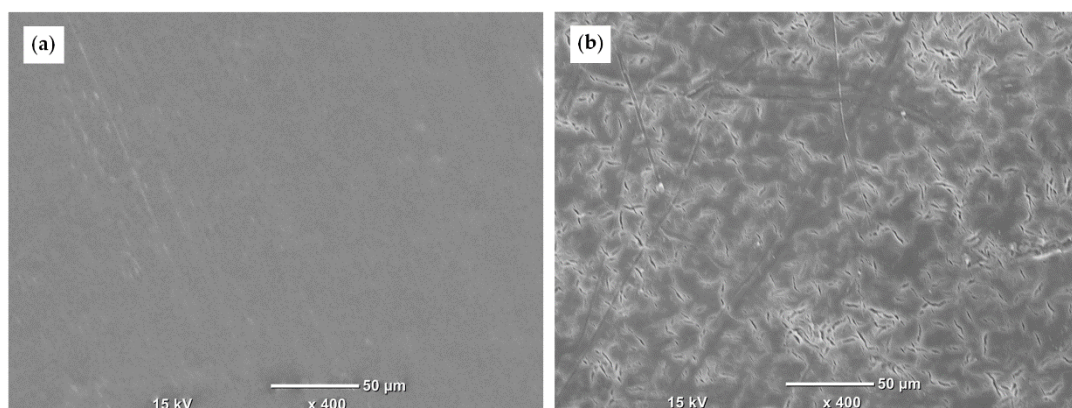


Figure 3. SEM images of the surfaces of polymer film **FB4** before (a) and after (b) 14 day hydrolysis in PBS.

As was demonstrated recently by Wurm et al. [14], in aqueous solution poly(EtOEP) undergoes relatively slow hydrolysis, the major hydrolytic degradation pathway is backbiting with the participation of polyphosphate chain ends— $\text{P}(\text{O})(\text{OEt})\text{CH}_2\text{CH}_2\text{OH}$. For copolymers obtained, such a mechanism seems even more likely. In our experiments, within 7 days for **FB4** (Figure 4a) a marked decrease in EtOEP content was detected (Figure 4b), however, after additional seven days, the $\epsilon\text{CL}/\text{EtOEP}$ ratio has changed little (Figure 4c). This can be attributed to superficial character of the hydrolysis affecting only poly(EtOEP) fragments, and lower hydrophilicity of the poly(ϵCL) surface formed.

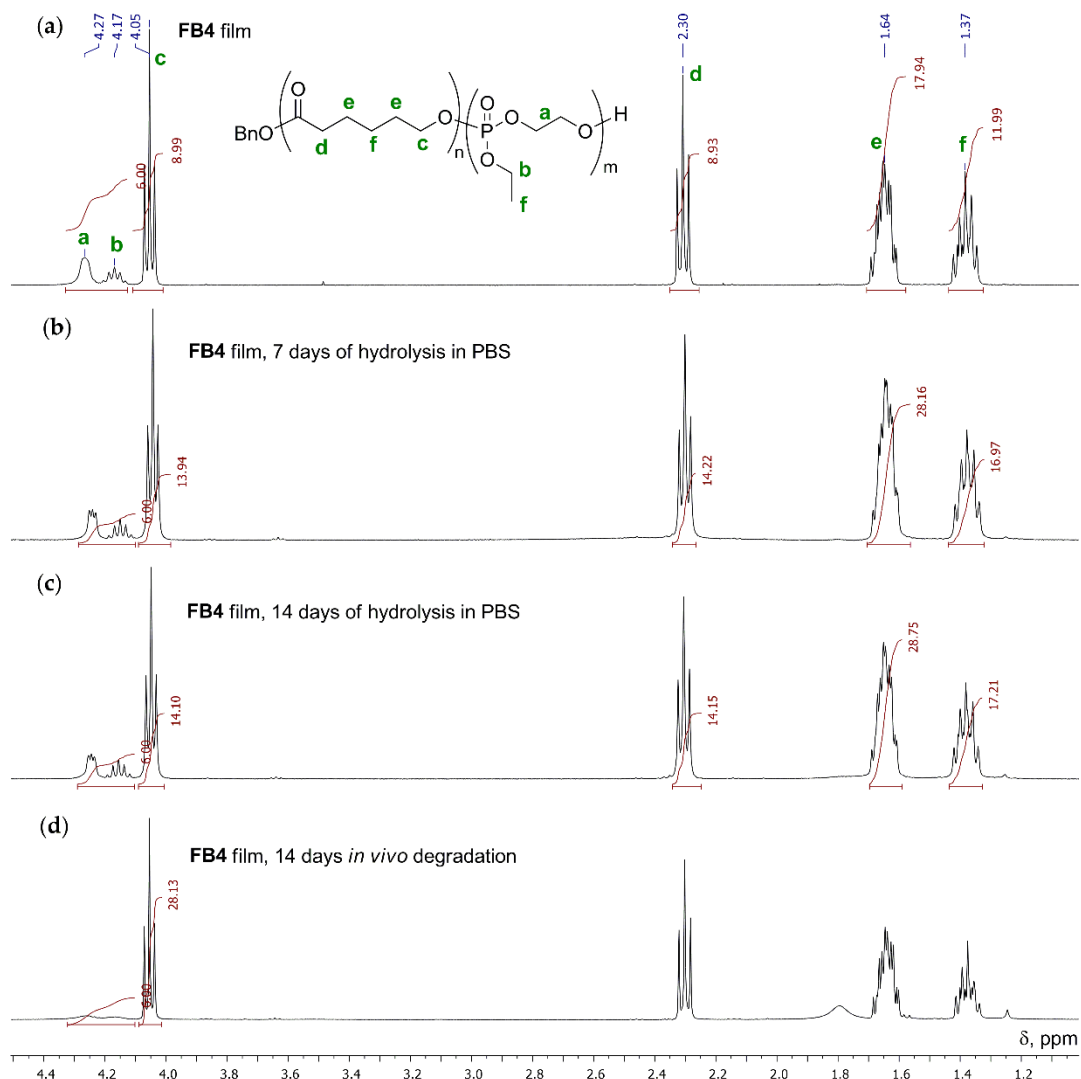


Figure 4. Hydrolytic degradation of FB4 film (a) *in vitro* (b,c) and *in vivo* (d).

3.4. Cytotoxicity

Cell viability was assessed by the MTT assay based on the ability of live cells to convert the water-soluble yellow 3-(4,5-dimethylthiazol-2-yl)-2,5-diphenyltetrazolium bromide (MTT) into insoluble purple intracellular crystals of MTT-formazan. The conversion efficiency is indicative of the general level of dehydrogenase activity of the cells under study, which is to a certain extent directly proportional to the concentration of viable cells [38]. The cytotoxicity test was conducted on the UC MSCs using the complete media extracts of FB1–FB4 films which were prepared by incubation of the film samples in the media containing 7.0×10^3 cells/well, followed by extraction and registration of UV–VIS spectra. Figure 5 shows the absorption intensities at $\lambda = 570$ nm for all samples after one, two, and four days of incubation. No significant differences were found in the comparison of the absorption intensity values of the extracts from UC MSCs-loaded wells with polymer film samples and extract from UC MSCs-loaded well without an addition of polymers (blue dotted line). Comparison of cell viability within the same film sample at different time points revealed no significant difference between one, two, and four days. In this way, FB1–FB4 demonstrated a complete absence of toxicity.

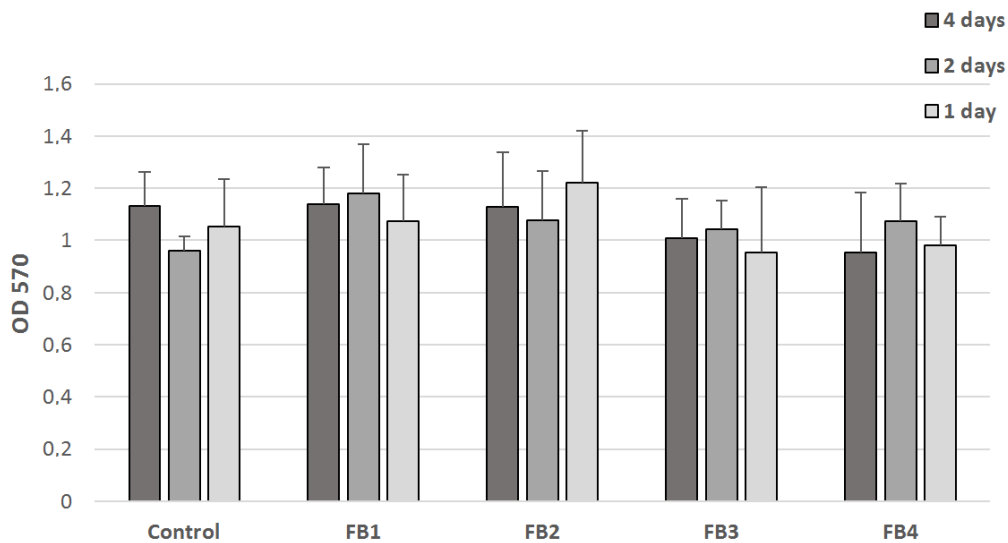


Figure 5. Evaluation of the cytotoxicity of polymer films **FB1–FB4** for UC MSCs: the results of MTT test after one, two, and four days of incubation.

3.5. Protein Adhesion

Protein adhesion is the process preceding cell adhesion. To compare the ability of the films **FB1–FB4** and **FB4'** to protein adhesion, the samples were incubated with GFP (see Section 2.4). Surface distribution of the adhered protein was analyzed using fluorescent microscopy (Figure 6). For poly(ϵ CL) film **FB1** we observed uniform protein coverage. With the increasing of EtOEP content, protein adhesion decreased. It is noteworthy that for **FB2** with relatively high ϵ CL/EtOEP GFP adhesion was uneven, exposing phosphate-free surface areas. For copolymer films with higher EtOEP content the cell adhesion was rare and spotty.

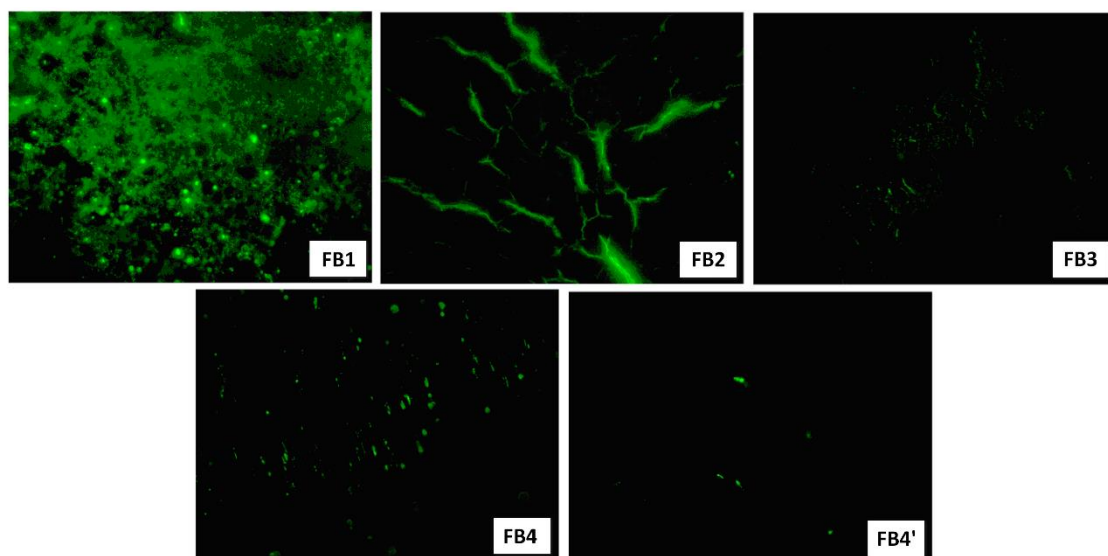


Figure 6. Adhesion of the GFP protein on the surface of the films **FB1–FB4** and **FB4'**. Fluorescent microscopy, magnification of 400 \times .

Therefore, even the minimal content of poly(ethylene phosphate) fragments in copolymer successfully prevent protein adhesion. For cell adhesion, we expected the same behavior.

3.6. Cell Adhesion and Cell Proliferation

Cell adhesion for **FB1–FB4** was studied using dynamic method of the seeding of UC MSCs (see Section 2.5). Cell count was evaluated based on the number of viable cells, stained with DAPI, that were adhered to the film surface (Figures 7 and 8, left). To observe the cell morphology, UC MSCs were labeled with a fluorescent red-orange vital dye PKH26 (Figure 8, right). Minor difference in cell adhesion was detected for **FB1** and **FB2**, but the presence of poly(EtOEP) fragments resulted in a lowering of the number of cells adhered. For copolymers with higher EtOEP content **P3** and **P4** minimal cell adhesion was detected.

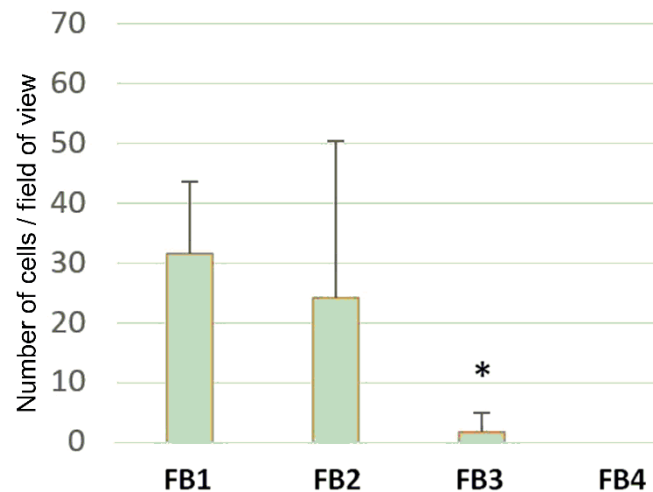


Figure 7. Evaluation of adhesive properties of polymer films **FB1–FB4** for UC MSCs (vertical scale—a number of cells in a field of view). * $p < 0.05$ in comparison with **FB-1**.

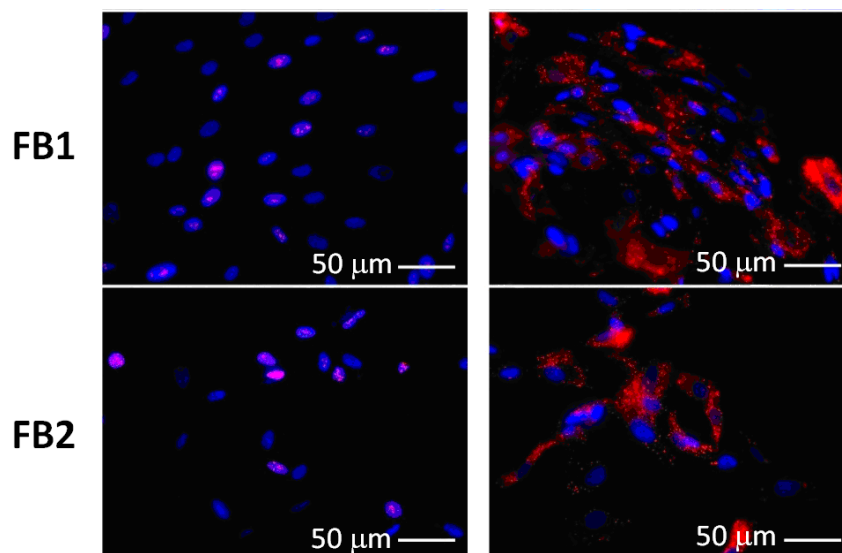


Figure 8. Evaluation of the rate of proliferating cells for UC MSCs (left) and cell morphology (right).

Immunocytochemical study showed a high level of the expression of proliferation marker Ki-67 in MSCs seeded on **FB1** and **FB2**, (Figure 8 right and Figure 9). A significantly lower rate of proliferating cells was detected for **FB3** and **FB4**.

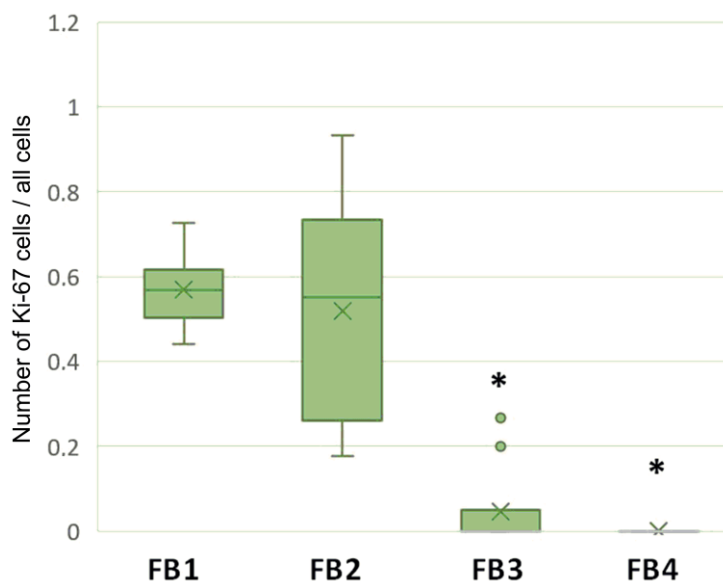


Figure 9. Evaluation of the proliferative properties of UC MSCs by the rate of Ki-67+ cells. * $p < 0.05$ in comparison with **FB-1**.

Summarizing the results of experiments on protein adhesion, cell adhesion, and cell proliferation, it can be concluded that even ~10% mol content of poly(ethylene phosphate) leads to almost complete suppression of these processes. In this way, on the example of poly(EtOEP) the efficiency of polyphosphate-based approach to anti-adhesive materials have been demonstrated. However, in vitro studies must be supplemented by in vivo studies that are able to reveal unknown side processes accompanying the use of novel polymer implants.

3.7. Subcutaneous Implantation Experiments

A connective tissue capsule was formed after subcutaneous implantation of all film samples. After 14 days, the thickness of the capsule around **FB4** sample was two times higher in comparison with **FB4'**, after additional two weeks the difference has almost disappeared (Figure 10). The least thickness of the capsule was detected for **FB1** and **FB2**. Thus, despite the explicit antiadhesive properties, copolymers with relatively high EtOEP content caused a rejection reaction. It can be assumed that this reaction is caused by the toxic response to acidic products [39] of the biodegradation of EtOEP-containing copolymers.

Analysis of ^1H NMR spectrum of **FB4** sample after 14 days of implantation (Figure 4d) showed three-quarters hydrolysis of the starting copolymer. Note that the rate of hydrolytic degradation in vivo was significantly higher than the rate of hydrolysis in PBS at the same temperature.

To assess the immune response during subcutaneous injection of the samples, a comparative analysis of the number of CD68+ cells was performed for the film/fibrous capsule border (Figure 11, Figure S6 in the Supplementary Materials). The highest CD68+ infiltration rate was detected after 14 days for **FB4**, 45.4 (31.3–78.7) cells/mm, for **FB4'** the value of 13.5 (10.6–15.7) cells/mm was detected (Figure 11). After 28 days, **FB4** was a leader (35.4 (31.6–36.9) cells/mm), the lowest infiltration was found for **FB1** (15.6 (9.4–24.5) cells/mm) (Figure 11). Thus, immune response was also grown with the increasing of the content of EtOEP in copolymer.

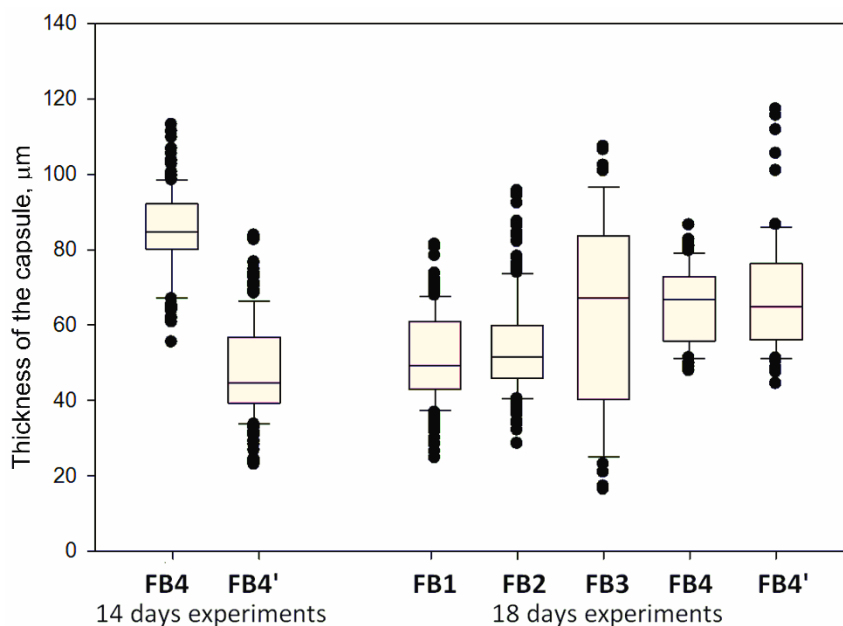


Figure 10. The thickness of the connective tissue capsule (μm) formed after subcutaneous implantation of the films FB1–FB4 and FB4'.

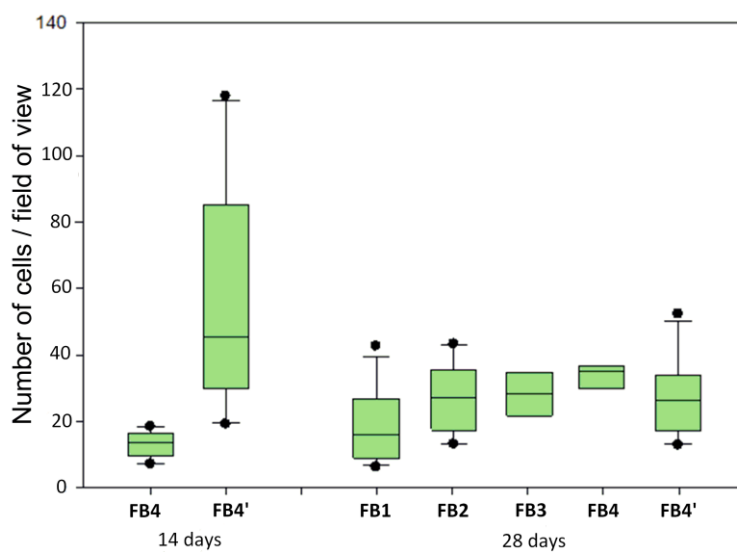


Figure 11. Number of CD68+ at the border of the polymer film and fibrous capsule.

4. Conclusions

At the beginning of the study it was suggested that poly(ethylene phosphate)s represent promising alternatives to PEG in the development of biomedical materials with antiadhesive properties. Using non-toxic BHT-Mg catalyst of coordination ROP, ϵCL homopolymer **P1** and three ϵCL /ethyl ethylene phosphate (EtOEP) block copolymers **P2–P4** with DP_n (ϵCL) ~ 200 and different ϵCL /EtOEP ratios have been prepared, and polymer films for the further studies on hydrolytic degradation and biocompatibility have been made.

It has been found that in vitro hydrolytic degradation of ϵCL /EtOEP block copolymers proceeds as a surface hydrolysis of polyphosphate fragments. This process was accompanied by the formation of extended caverns (peculiar ‘chemical crazing’). As expected, ϵCL /EtOEP block copolymers demonstrated anti-adhesive properties against proteins (GFP) and cells (MSCs). However, subcutaneous implantation experiments showed that poly(EtOEP)-containing films cause the formation

of fibrous capsules, presumably due to response on the formation of acidic products during the hydrolysis of polyphosphate.

The results of these studies can be used for the further development of biocompatible and biodegradable materials for tissue engineering and other biomedical applications. It can be assumed that negative response, detected during in vivo experiments, can be mitigated by the use of basic components in formulations of the prospective polymer composites.

Supplementary Materials: The following are available online at <http://www.mdpi.com/2073-4360/12/12/3039/s1>, **Figure S1.** ¹H NMR spectrum (400 MHz, CDCl₃, 20 °C) of εCL homopolymer **P1**; **Figure S2.** ¹H NMR spectrum (400 MHz, CDCl₃, 20 °C) of copolymer **P2**; **Figure S3.** ¹H NMR spectrum (400 MHz, CDCl₃, 20 °C) of copolymer **P3**; **Figure S4.** ¹H NMR spectrum (400 MHz, CDCl₃, 20 °C) of copolymer **P4**; **Figure S5.** Connective tissue capsules after 28 days after subcutaneous administration of the polymer films. Stained by hematoxylin and eosin, line segment 100 μm; **Figure S6.** CD68+ cells at the border between fibrous capsule and film. Immunocytochemical stain, fluorescent microscopy, cell nuclei stained by DAPI, line segment 50 μm.

Author Contributions: Conceptualization: I.N. and T.F.; methodology: A.E. and P.I.; software: A.E.; validation: I.N., A.E., and T.F.; formal analysis: E.K.; investigation: A.S., P.K., A.T., E.K., A.E., and P.V.; resources: I.N., A.E., and T.F.; data curation: T.F.; writing—original draft preparation: P.I.; writing—review and editing: E.K., T.F., and P.I.; visualization: E.K. and P.I.; supervision: I.N. and T.F.; project administration: I.N.; funding acquisition: I.N. All authors have read and agreed to the published version of the manuscript.

Funding: This research was funded by the Russian Science Foundation, grant number 16-13-10344, and was carried out within the State Program of TIPS RAS (as part of polymer analysis).

Acknowledgments: The authors are grateful for the exploitation of the equipment of the TIPS RAS Center of Collective Use: “New Petrochemical Processes, Polymer Composites and Adhesives”.

Conflicts of Interest: The authors declare no conflict of interest.

References

1. Schulte, V.A.; Díez, M.; Möller, M.; Lensen, M.C. Surface Topography Induces Fibroblast Adhesion on Intrinsically Nonadhesive Poly(ethylene glycol) Substrates. *Biomacromolecules* **2009**, *10*, 2795–2801. [[CrossRef](#)]
2. Nair, A.; Zou, L.; Bhattacharyya, D.; Timmons, R.B.; Tang, L. Species and Density of Implant Surface Chemistry Affect the Extent of Foreign Body Reactions. *Langmuir* **2008**, *24*, 2015–2024. [[CrossRef](#)]
3. Chen, H.; Yuan, L.; Song, W.; Wu, Z.; Li, D. Biocompatible polymer materials: Role of protein–surface interactions. *Prog. Polym. Sci.* **2008**, *33*, 1059–1087. [[CrossRef](#)]
4. Ngo, B.K.D.; Grunlan, M.A. Protein Resistant Polymeric Biomaterials. *ACS Macro Lett.* **2017**, *6*, 992–1000. [[CrossRef](#)]
5. Pelosi, C.; Tinè, M.R.; Wurm, F.R. Main-chain water-soluble polyphosphoesters: Multi-functional polymers as degradable PEG-alternatives for biomedical applications. *Eur. Polym. J.* **2020**, *141*, 110079. [[CrossRef](#)]
6. Abraham, A.A.; Means, A.K.; Clubb, F.J., Jr.; Fei, R.; Locke, A.K.; Gacasan, E.G.; Coté, G.L.; Grunlan, M.A. Foreign Body Reaction to a Subcutaneously Implanted Self-Cleaning, Thermoresponsive Hydrogel Membrane for Glucose Biosensors. *ACS Biomater. Sci. Eng.* **2018**, *4*, 4104–4111. [[CrossRef](#)]
7. Wang, Y.-C.; Yuan, Y.-Y.; Du, J.-Z.; Yang, X.-Z.; Wang, J. Recent progress in polyphosphoesters: From controlled synthesis to biomedical applications. *Macromol. Biosci.* **2009**, *9*, 1154–1164. [[CrossRef](#)]
8. Penczek, S.; Pretula, J.B.; Kaluzynski, K.; Lapienis, G. Polymers with Esters of Phosphoric Acid Units: From Synthesis, Models of Biopolymers to Polymer–Inorganic Hybrids. *Isr. J. Chem.* **2012**, *52*, 306–319. [[CrossRef](#)]
9. Steinbach, T.; Wurm, F.R. Poly(phosphoester)s: A new platform for degradable polymers. *Angew. Chem. Int. Ed.* **2015**, *54*, 6098–6108. [[CrossRef](#)]
10. Yilmaz, Z.E.; Jérôme, C. Polyphosphoesters: New trends in synthesis and drug delivery applications. *Macromol. Biosci.* **2016**, *16*, 1745–1761. [[CrossRef](#)]
11. Nifant'ev, I.E.; Shlyakhtin, A.V.; Bagrov, V.V.; Komarov, P.D.; Kosarev, M.A.; Tavtorkin, A.N.; Minyaev, M.E.; Roznyatovsky, V.A.; Ivchenko, P.V. Controlled ring-opening polymerisation of cyclic phosphates, phosphonates and phosphoramidates catalysed by heteroleptic BHT-alkoxy magnesium complexes. *Polym. Chem.* **2017**, *8*, 6806–6816. [[CrossRef](#)]
12. Bauer, K.N.; Tee, H.T.; Velencoso, M.M.; Wurm, F.R. Main-chain poly(phosphoester)s: History, syntheses, degradation, bio- and flame-retardant applications. *Prog. Polym. Sci.* **2017**, *73*, 61–122. [[CrossRef](#)]

13. Becker, G.; Wurm, F.R. Functional biodegradable polymers via ring-opening polymerization of monomers without protective groups. *Chem. Soc. Rev.* **2018**, *47*, 7739–7782. [[CrossRef](#)]
14. Bauer, K.N.; Liu, L.; Wagner, M.; Andrienko, D.; Wurm, F.R. Mechanistic study on the hydrolytic degradation of polyphosphates. *Eur. Polym. J.* **2018**, *108*, 286–294. [[CrossRef](#)]
15. Wang, Y.-C.; Liu, X.-Q.; Sun, T.-M.; Xiong, M.-H.; Wang, J. Functionalized micelles from block copolymer of polyphosphoester and poly(ϵ -caprolactone) for receptor-mediated drug delivery. *J. Contr. Release* **2008**, *128*, 32–40. [[CrossRef](#)]
16. Steinbach, T.; Becker, G.; Spiegel, A.; Figueiredo, T.; Russo, D.; Wurm, F.R. Reversible bioconjugation: Biodegradable poly(phosphate)-protein conjugates. *Macromol. Biosci.* **2017**, *17*, 1600377. [[CrossRef](#)]
17. Pelosi, C.; Duce, C.; Russo, D.; Tiné, M.R.; Wurm, F.R. PPEylation of proteins: Synthesis, activity, and stability of myoglobin-polyphosphoester conjugates. *Eur. Polym. J.* **2018**, *108*, 357–363. [[CrossRef](#)]
18. Zhai, X.; Huang, W.; Liu, J.; Pang, Y.; Zhu, X.; Zhou, Y.; Yan, D. Micelles from amphiphilic block copolyphosphates for drug delivery. *Macromol. Biosci.* **2011**, *11*, 1603–1610. [[CrossRef](#)]
19. McKinlay, C.J.; Waymouth, R.M.; Wender, P.A. Cell-Penetrating, Guanidinium-Rich Oligophosphoesters: Effective and Versatile Molecular Transporters for Drug and Probe Delivery. *J. Am. Chem. Soc.* **2016**, *138*, 3510–3517. [[CrossRef](#)]
20. Zhang, F.; Zhang, S.; Pollack, S.F.; Li, R.; Gonzalez, A.M.; Fan, J.; Zou, J.; Leininger, S.E.; Pavia-Sanders, A.; Johnson, R.; et al. Improving paclitaxel delivery: In vitro and in vivo characterization of PEGylated polyphosphoester-based nanocarriers. *J. Am. Chem. Soc.* **2015**, *137*, 2056–2066. [[CrossRef](#)]
21. Schöttler, S.; Becker, G.; Winzen, S.; Steinbach, T.; Mohr, K.; Landfester, K.; Mailänder, V.; Wurm, F.R. Protein adsorption is required for stealth effect of poly(ethylene glycol)- and poly(phosphoester)-coated nanocarriers. *Nat. Nanotech.* **2016**, *11*, 372–377. [[CrossRef](#)] [[PubMed](#)]
22. Pranantyo, D.; Xu, L.Q.; Kang, E.-T.; Mya, M.K.; Chan-Park, M.B. Conjugation of polyphosphoester and antimicrobial peptide for enhanced bactericidal activity and biocompatibility. *Biomacromolecules* **2016**, *17*, 4037–4044. [[CrossRef](#)] [[PubMed](#)]
23. Chew, S.Y.; Mi, R.; Hoke, A.; Leong, K.W. Aligned Protein–Polymer Composite Fibers Enhance Nerve Regeneration: A Potential Tissue-Engineering Platform. *Adv. Funct. Mater.* **2007**, *17*, 1288–1296. [[CrossRef](#)] [[PubMed](#)]
24. Yang, X.-Z.; Sun, T.-M.; Dou, S.; Wu, J.; Wang, Y.-C.; Wang, J. Block Copolymer of Polyphosphoester and Poly(L-Lactic Acid) Modified Surface for Enhancing Osteoblast Adhesion, Proliferation, and Function. *Biomacromolecules* **2009**, *10*, 2213–2220. [[CrossRef](#)]
25. Arbaoui, A.; Redshaw, C. Metal catalysts for ϵ -caprolactone polymerisation. *Polym. Chem.* **2010**, *1*, 801–826. [[CrossRef](#)]
26. Nifant'ev, I.E.; Shlyakhtin, A.V.; Bagrov, V.V.; Minyaev, M.E.; Churakov, A.V.; Karchevsky, S.G.; Birin, K.P.; Ivchenko, P.V. Mono-BHT heteroleptic magnesium complexes: Synthesis, molecular structure and catalytic behavior in the ring-opening polymerization of cyclic esters. *Dalton Trans.* **2017**, *46*, 12132–12146. [[CrossRef](#)]
27. Steinbach, T.; Schröder, R.; Ritz, S.; Wurm, F.R. Microstructure analysis of biocompatible phosphoester copolymers. *Polym. Chem.* **2013**, *4*, 4469–4479. [[CrossRef](#)]
28. Li, J.; Stayshich, R.M.; Meyer, T.Y. Exploiting Sequence to Control the Hydrolysis Behavior of Biodegradable PLGA Copolymers. *J. Am. Chem. Soc.* **2011**, *133*, 6910–6913. [[CrossRef](#)]
29. Pogorielov, M.; Hapchenko, A.; Deineka, V.; Rogulska, L.; Oleshko, O.; Vodsed'álková, K.; Berezkinová, L.; Vysloužilová, L.; Klápšťová, A.; Erben, J. In vitro degradation and in vivo toxicity of NanoMatrix3D[®] polycaprolactone and poly(lactic acid) nanofibrous scaffolds. *J. Biomed. Mater. Res.* **2018**, *106*, 2200–2212. [[CrossRef](#)]
30. Mushahary, D.; Spittler, A.; Kasper, C.; Weber, V.; Charwat, V. Isolation, cultivation, and characterization of human mesenchymal stem cells. *J. Quant. Cell Sci.* **2018**, *93*, 19–31. [[CrossRef](#)]
31. Lamanna, R.; Corti, A.; Iorio, M.; Nocchi, F.; Urciuoli, P.; Lapi, S.; Scatena, F.; Franzini, M.; Vanacore, R.; Lorenzini, E.; et al. Are standard cell culture conditions adequate for human umbilical cord blood mesenchymal stem cells? *Blood Transfus.* **2014**, *12*, s375–s377. [[CrossRef](#)] [[PubMed](#)]
32. Nifant'ev, I.E.; Shlyakhtin, A.V.; Tavtorkin, A.N.; Ivchenko, P.V.; Borisov, R.S.; Churakov, A.V. Monomeric and dimeric magnesium mono-BHT complexes as effective ROP catalysts. *Catal. Commun.* **2016**, *87*, 106–111. [[CrossRef](#)]

33. Nifant'ev, I.E.; Shlyakhtin, A.V.; Bagrov, V.V.; Komarov, P.D.; Kosarev, M.A.; Tavtorkin, A.N.; Minyaev, M.E.; Roznyatovsky, V.A.; Ivchenko, P.V. Synthesis and ring-opening polymerization of glycidyl ethylene phosphate with a formation of linear and branched polyphosphates. *Mendeleev Commun.* **2018**, *28*, 155–157. [[CrossRef](#)]
34. Nifant'ev, I.E.; Shlyakhtin, A.V.; Bagrov, V.V.; Komarov, P.D.; Tavtorkin, A.N.; Minyaev, M.E.; Kosarev, M.A.; Ivchenko, P.V. Synthesis in aqueous media of poly(ethylene phosphoric acids) by mild thermolysis of homopolymers and block copolymers based on *tert*-butyl ethylene phosphate. *Eur. Polym. J.* **2018**, *106*, 249–256. [[CrossRef](#)]
35. Nifant'ev, I.; Shlyakhtin, A.; Kosarev, M.; Karchevsky, S.; Ivchenko, P. Mechanistic Insights of BHT-Mg-Catalyzed Ethylene Phosphate's Coordination Ring-Opening Polymerization: DFT Modeling and Experimental Data. *Polymers* **2018**, *10*, 1105. [[CrossRef](#)]
36. Nifant'ev, I.; Shlyakhtin, A.; Kosarev, M.; Gavrilov, D.; Karchevsky, S.; Ivchenko, P. DFT Visualization and Experimental Evidence of BHT-Mg-Catalyzed Copolymerization of Lactides, Lactones and Ethylene Phosphates. *Polymers* **2019**, *11*, 1641. [[CrossRef](#)]
37. Kosarev, M.A.; Gavrilov, D.E.; Nifant'ev, I.E.; Shlyakhtin, A.V.; Tavtorkin, A.N.; Dyadchenko, V.P.; Roznyatovsky, V.A.; Ivchenko, P.V. Ultrafast hydrolytic degradation of 2,3-dihydroxypropyl functionalized poly(ethylene phosphates). *Mendeleev Commun.* **2019**, *29*, 509–511. [[CrossRef](#)]
38. Pannecouque, C.; Daelemans, D.; De Clercq, E. Tetrazolium-based colorimetric assay for the detection of HIV replication inhibitors: Revisited 20 years later. *Nat. Protoc.* **2008**, *3*, 427–434. [[CrossRef](#)]
39. Hakkarainen, M.; Höglund, A.; Odelius, K.; Albertsson, A.-C. Tuning the Release Rate of Acidic Degradation Products through Macromolecular Design of Caprolactone-Based Copolymers. *J. Am. Chem. Soc.* **2007**, *129*, 6308–6312. [[CrossRef](#)]

Publisher's Note: MDPI stays neutral with regard to jurisdictional claims in published maps and institutional affiliations.



© 2020 by the authors. Licensee MDPI, Basel, Switzerland. This article is an open access article distributed under the terms and conditions of the Creative Commons Attribution (CC BY) license (<http://creativecommons.org/licenses/by/4.0/>).